



OPEN

MSU crystallization promotes fibroblast proliferation and renal fibrosis in diabetic nephropathy via the ROS/SHP2/TGF β pathway

Jing Li^{1,4}, Jiwei Zhang^{2,4}, Xuying Zhao³✉ & Ling Tian¹✉

Monosodium urate (MSU) crystallisation deposited in local tissues and organs induce inflammatory reactions, resulting in diseases such as gout. MSU has been recognized as a common and prevalent pathology in various clinical conditions. In this study, we investigated the role of MSU in the pathogenesis of diabetic kidney disease (DKD). We induced renal injury in diabetic kidney disease mice using streptozotocin (STZ) and assessed renal histopathological damage using Masson's trichrome staining and Collagen III immunofluorescence staining. We measured the levels of malondialdehyde (MDA), superoxide dismutase (SOD), and uric acid (UA) using ELISA. Protein expression levels of NLRP3, p-NF- κ B, SHP2, p-STAT3, and p-ERK1/2 were analyzed by Western blot. To further investigate the role of MSU in diabetic kidney disease, we conducted in vitro experiments. In our in vivo experiments, we found that compared to the Model group, there was a significant increase in interstitial fibrosis in the kidneys of mice after treatment with MSU, accompanied by elevated levels of MDA, SOD, and UA. Furthermore, the protein expression of NLRP3, p-NF- κ B, SHP2, p-STAT3, and p-ERK1/2 was upregulated. In our subsequent studies on mouse fibroblasts (L929 cells), we discovered that high glucose, MSU, and TGF- β could promote the expression of P22, GP91, NLRP3, NF- κ B, p-NF- κ B, p-SHP2, p-EGFR, p-STAT3, and Collagen-III proteins. Additionally, we found that SHP2 could counteract the upregulation trend induced by MSU on the expression of p-SHP2, p-EGFR, p-STAT3, and Collagen-III proteins, and inhibitors YQ128, NAC, and Cetuximab exhibited similar effects. Furthermore, immunofluorescence results indicated that SHP2 could inhibit the expression of the fibrosis marker α -SMA in L929 cells. These findings suggest that MSU can promote renal fibroblast SHP2 expression, induce oxidative stress, activate the NLRP3/NF- κ B pathway, and enhance diabetic kidney disease fibroblast proliferation through the TGF β /STAT3/ERK1/2 signaling pathway, leading to renal fibrosis.

Keywords Diabetic kidney disease, Fibrosis, ROS, SHP2, NLRP3, STAT3

In recent years, diabetic kidney disease (DKD) has become one of the most common and severe complications in patients with diabetes worldwide. The global prevalence of diabetes is rapidly increasing, especially in developing countries^{1,2}. It not only has a significant impact on the quality of life of patients but also increases the risk of developing chronic kidney disease and end-stage renal failure, as its complications include long-term dysfunction and organ failure¹. Although several studies have investigated the pathogenesis of DKD³⁻⁵, there are still many unanswered questions, particularly regarding the role of MSU crystallisation in renal fibrosis⁶.

The molecular formula of monosodium urate (MSU) is C₅H₅N₄NaO₃. High levels of uric acid in the blood are likely to lead to the deposition of monosodium urate (MSU). Studies have confirmed that uric acid (UA) crystallisation plays a key role in inflammatory reaction as the main pathogenic factor in diseases like gout^{7,8}. Furthermore, MSU crystallisation is increasingly recognized as a risk factor that may have a significant impact on the development of DKD⁹. Complex molecular mechanisms and cell signaling pathways regulate the role of

¹Department of Nephrology, Affiliated Hospital of Hebei University, 212 Yuhua East Road, Baoding, China. ²Department of Cardiovascular Medicine, Affiliated Hospital of Hebei University, Baoding, China. ³Department of Endocrinology, Affiliated Hospital of Hebei University, 212 Yuhua East Road, Baoding, China. ⁴These authors contributed equally: Jing Li and Jiwei Zhang. ✉email: lxy113194280@sina.com; lliuliulialice@sina.com

MSU crystallisation in DKD, with oxidative stress and imbalance in the SHP2/TGF β pathway considered to be an important regulatory mechanism in the pathogenesis of DKD^{10–12}.

The NLRP3 inflammasome is crucial in immune and inflammatory responses, and its excessive activation has been detected in various human diseases, such as diabetic cardiomyopathy, atherosclerosis, and autoimmune diseases^{13–15}. The activation of the NLRP3 inflammasome requires the signaling of NF- κ B as a prerequisite¹⁶. NF- κ B signaling is a crucial transcription factor that plays a vital role in inflammation and immunity. NF- κ B also has important roles in other processes, including development, cell growth, survival, and proliferation, and is involved in many pathological conditions. NF- κ B has been proposed as an oxidant-sensing transcription factor activated by ROS, and ROS can have various stimulatory effects on NF- κ B signaling¹⁷.

The aim of this study is not only to further understand the role of MSU crystallisation in the pathogenesis of DKD but also to provide new theoretical basis and clinical guidance for the diagnosis, treatment, and prevention of DKD. By elucidating the association between MSU crystallisation and renal fibrosis, we hope to provide new insights for the development of therapeutic strategies targeting this process and contribute to improving the prognosis of DKD patients.

Materials and methods

Animal model

This study was conducted in accordance with the ARRIVE guidelines and approved by the Ethics Committee of Academic Committee of Hebei North University (HBNU2023041022758). All the processes are in strict accordance with the National Institutes of Health (NIH) Guide for the Care and Use of Animals in laboratory experiments. C57BL/6 J mice were purchased from Henan Sk-bio Biotechnology Co., Ltd. The mice were housed in a specific pathogen-free (SPF) animal facility with a temperature controlled at 25 \pm 2 $^{\circ}$ C. The facility had a 12:12 light–dark cycle, and the mice had ad libitum access to food and water. After one week of acclimatization, the mice were randomly divided into three groups: sham group (healthy mice, n = 6), Model group (n = 6), and MSU group (n = 6). Based on previous studies, the mice in the experimental and MSU groups were induced to develop DKD by daily intraperitoneal injection of streptozotocin (STZ, 50 mg/kg) for five consecutive days¹⁸. The mice in the MSU group were intravenously injected with MSU crystals (50 mg/kg, dissolved in 1 \times PBS). The control and Model groups were injected with equal amounts of PBS solution. After 24 h, the mice were euthanized under sodium pentobarbital anesthesia (40 mg/kg) by cervical dislocation, and the kidney tissues were collected for biochemical and histopathological assessment.

Histological staining of animal tissues

The kidney tissues were fixed in 4% paraformaldehyde and embedded in paraffin for histological staining using Masson's trichrome staining and immunofluorescence. Briefly, the kidney tissues were sectioned into 4 μ m thick slices and rehydrated using a series of ethanol solutions with varying concentrations. Masson's trichrome staining was performed using the Modified Masson's Trichrome Stain Kit (Solarbio). The slices were stained with Weigert's iron hematoxylin for 2 min, followed by ponceau-acid fuchsin stain for 10 min, and then aniline blue stain for 5 min. Finally, the slices were dehydrated with ethanol. For Collagen III immunofluorescence staining, the slices were treated with citrate buffer (0.01 M, pH 6) in a pressure cooker for antigen retrieval, followed by inactivation of endogenous peroxidase with 3% H₂O₂. The slices were then incubated overnight at 4 $^{\circ}$ C with primary antibody against Collagen III (1/1000, abcam, ab184993), followed by incubation with fluorescent secondary antibody (1:500, abcam, ab150081) at room temperature in a dark environment. The staining was observed under a fluorescence microscope.

ELISA

The kidney tissues were homogenized in cold 0.9% saline, and the supernatant was collected after centrifugation. The levels of superoxide dismutase (SOD), malondialdehyde (MDA), and uric acid (UA) in the kidney tissue homogenate were measured according to the manufacturer's instructions of the ELISA kits. The SOD activity was measured using the Superoxide Dismutase (SOD) Colorimetric Activity Assay Kit (EIASODC, Thermo Fisher Scientific Inc.). The UA content was measured using the Uric Acid Assay Kit (BC1365, Solarbio). Every result was issued from three independent experiments.

Western blot

The kidney tissues were lysed in radioimmunoprecipitation assay (RIPA) buffer (Solarbio), and the samples were collected by centrifugation at 12,000 rpm, 4 $^{\circ}$ C. The protein concentration of the samples was determined using the BCA assay. The proteins were separated by SDS-PAGE and transferred onto PVDF membranes. After blocking with 5% skim milk, the membranes were incubated overnight at 4 $^{\circ}$ C with primary antibodies against NLRP3 (1:1000, abcam, ab263899), p-NF- κ B (1:1000, Cell Signaling Technology, Inc., 3031 s), SHP2 (1:1000, abcam, ab300579), p-STAT3 (1:1000, abcam, ab97051), p-ERK1/2 (1:1000, abcam, ab97051), P22 (1:1000, abcam, pT202/Y204), gp91 (1:1000, abcam, ab310337), p-SHP2 (1:1000, abcam, ab62322), p-EGFR (1:1000, abcam, ab40815), NF- κ B (1:1000, abcam, ab32536), Collagen III (1:1000, abcam, ab184993), and GAPDH (1:1000, abcam, ab263899). After incubation with HRP-conjugated anti-rabbit secondary antibody at room temperature for 1 h, the membranes were developed using an enhanced chemiluminescence substrate and quantified using ImageJ software.

Cell culture and cell proliferation assay

Cell culture and treatment: L929 murine fibroblast cell line was obtained from Thermo Fisher Scientific Inc. The cells were cultured in RPMI 1640 medium supplemented with 10% fetal bovine serum, 2 mM L-glutamine, 100

U/mL penicillin, and 100 µg/mL streptomycin at 37 °C in a humidified atmosphere of 5% CO₂. After passaging, the cells were cultured in high glucose medium (50 mM) for the experimental group, while the sham group was cultured in regular medium. The cells were stimulated with MSU crystals (200 µg/mL) for 5 h¹⁹. For NLRP3 inhibition, the cells in the NLRP3 inhibition group were cultured with MCC950 (8.1 nM). Regarding ROS inhibition cells were treated using 3 mM NAC. SHP2-specific shRNA was obtained from GenePharma. L929 cells were transfected with SHP2-specific shRNA using Lipofectamine 3000. After 48 h of transfection, the culture medium was replaced with fresh medium, and the experiment was continued. For EGFR inhibition, the cells were treated with cetuximab (100 µg/ml) for 24 h. Regarding the cellular model of combined TGF-β and high glucose induction, 2 ng/ml of TGF-β was added to high glucose medium and the cells were treated for 24 h²⁰.

Cell proliferation assay and immunofluorescence: Single-cell suspensions were added onto coverslips in a 6-well plate and cultured at 37 °C, 5% CO₂ for 24 h. The coverslips were then removed from the culture plate, and the cells were fixed in 4% paraformaldehyde for 30 min and blocked with 5% goat serum at room temperature for 30 min. The cells were then incubated with primary antibody against α-SMA (abcam) overnight at 4 °C, followed by incubation with fluorescent secondary antibody (1:500, abcam, ab150081) at room temperature in a dark environment for 1 h. The staining was observed under a fluorescence microscope.

Statistical analysis

Statistical analysis was performed using GraphPad Prism 6. The results are presented as mean ± standard deviation (S.D). Independent samples t-test or two-way ANOVA were used for comparisons between different groups. P < 0.05 was considered statistically significant (Supplementary Table 1, Supplementary Table 2).

Ethics statement

This study was approved by the Ethics Committee of Academic Committee of Hebei North University (HBNU2023041022758).

Results

The impact of MSU on diabetic nephropathy lesions

We revealed renal fibrosis in diabetic mice through Masson's trichrome staining. Compared to the sham group, the model group of diabetic mice showed renal fibrosis (blue) in the Masson staining results. Furthermore, compared to the model group, MSU treatment resulted in more severe collagen fibrosis and infiltration of inflammatory cells in diabetic mice. (Fig. 1).

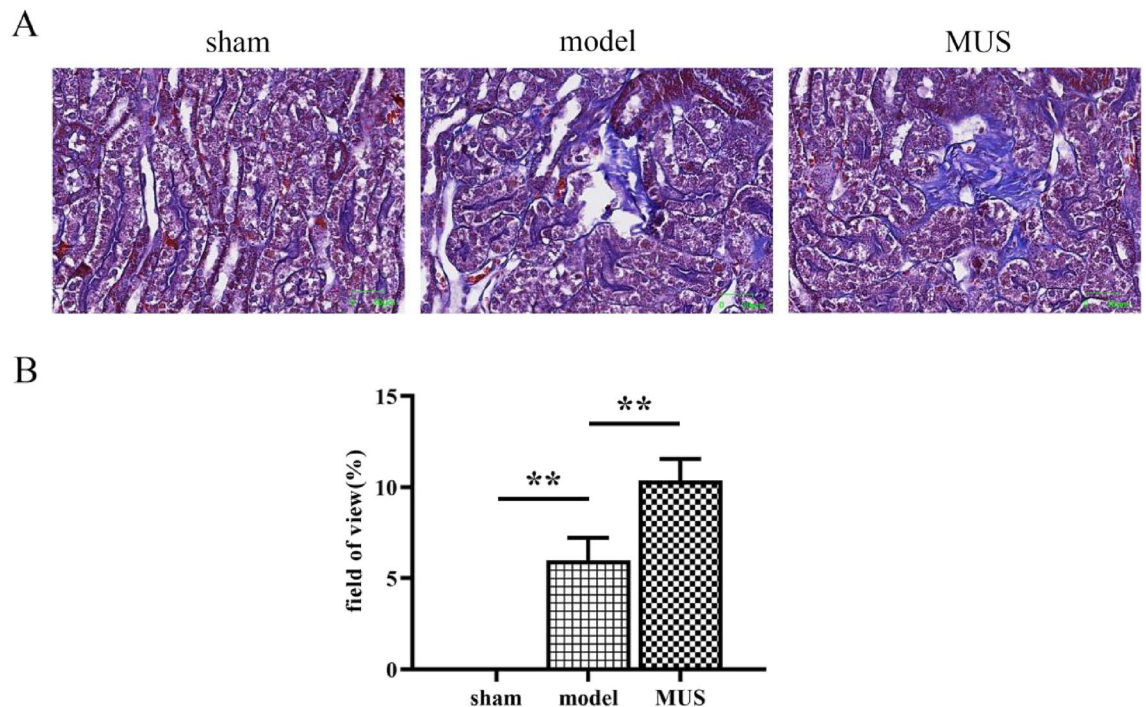


Figure 1. MSU exacerbates renal fibrosis in diabetic nephropathy mice. (A) Representative microscopic images of renal fibrosis in mice using Masson's staining. (B) Bar graph measuring collagen protein content using Masson's staining. **P < 0.01.

The effects of MSU on the ROS/SHP2 pathway and expression of fibrosis-related proteins in diabetic nephropathy mice

ELISA analysis showed that MSU elevated levels of ROS markers such as MDA, SOD, and UA. To further investigate the ROS-related pathway and expression of fibrosis-related proteins in mice, the expression of NLRP3, p-NF- κ B, SHP2, p-STAT3, and p-ERK1/2 was detected. Compared to the sham group, diabetic mice exhibited upregulation of NLRP3, p-NF- κ B, SHP2, p-STAT3, and p-ERK1/2 protein expression. MSU further promoted the expression of NLRP3, p-NF- κ B, SHP2, p-STAT3, and p-ERK1/2 proteins in diabetic mice. (Fig. 2).

The effects of NAC, MCC950, and MSU on oxidative stress-related protein expression in high-glucose-induced L929 cells

We found that compared to L929 fibroblasts cultured in normal medium, the protein expression of P22, GP91, NLRP3, p-NF- κ B, and SHP2 was upregulated under high-glucose conditions. MSU promoted the protein expression of P22, GP91, NLRP3, p-NF- κ B, and SHP2 in L929 cells under high-glucose conditions. The NLRP3 inhibitor, MCC950, inhibited the protein expression of P22, GP91, NLRP3, p-NF- κ B, and SHP2 in high-glucose and MSU-stimulated L929 cells. Similarly, the ROS inhibitor, NAC, inhibited the protein expression of P22 and SHP2 in high-glucose and MSU-stimulated L929 cells. These results suggest that MSU promotes renal fibrosis by activating the NLRP3/ROS signaling pathway to induce SHP2 expression. (Fig. 3).

The effects of SHP2, MCC950, and Cetuximab on the expression of related proteins in high-glucose-induced L929 cells

Stimulating L929 cells cultured under high-glucose conditions with TGF β , we found that MCC950 inhibited the protein expression of NLRP3, P22, NF- κ B, SHP2, p-SHP2, p-EGFR, p-ERK1/2, and p-STAT3. After treatment with the EGFR inhibitor, Cetuximab, the protein expression of p-EGFR, p-ERK1/2, and p-STAT3 was down-regulated. Knocking down SHP2 resulted in decreased protein expression of p-SHP2, p-EGFR, p-ERK1/2, and p-STAT3. MSU significantly promoted the protein expression of NLRP3, P22, NF- κ B, p-NF- κ B, SHP2, p-SHP2, p-EGFR, p-ERK1/2, and p-STAT3. In a comparison of the combined effect of MCC950 and MSU with the stimulation of MCC950 alone, we found that there was no significant difference in the protein expression levels of NLRP3, P22, NF- κ B, SHP2, p-SHP2, p-EGFR, p-ERK1/2, and p-STAT3 in the L929 cells under the combined action of MCC950 and MSU ($P > 0.05$). Under the combination effect of Cetuximab and MSU, there

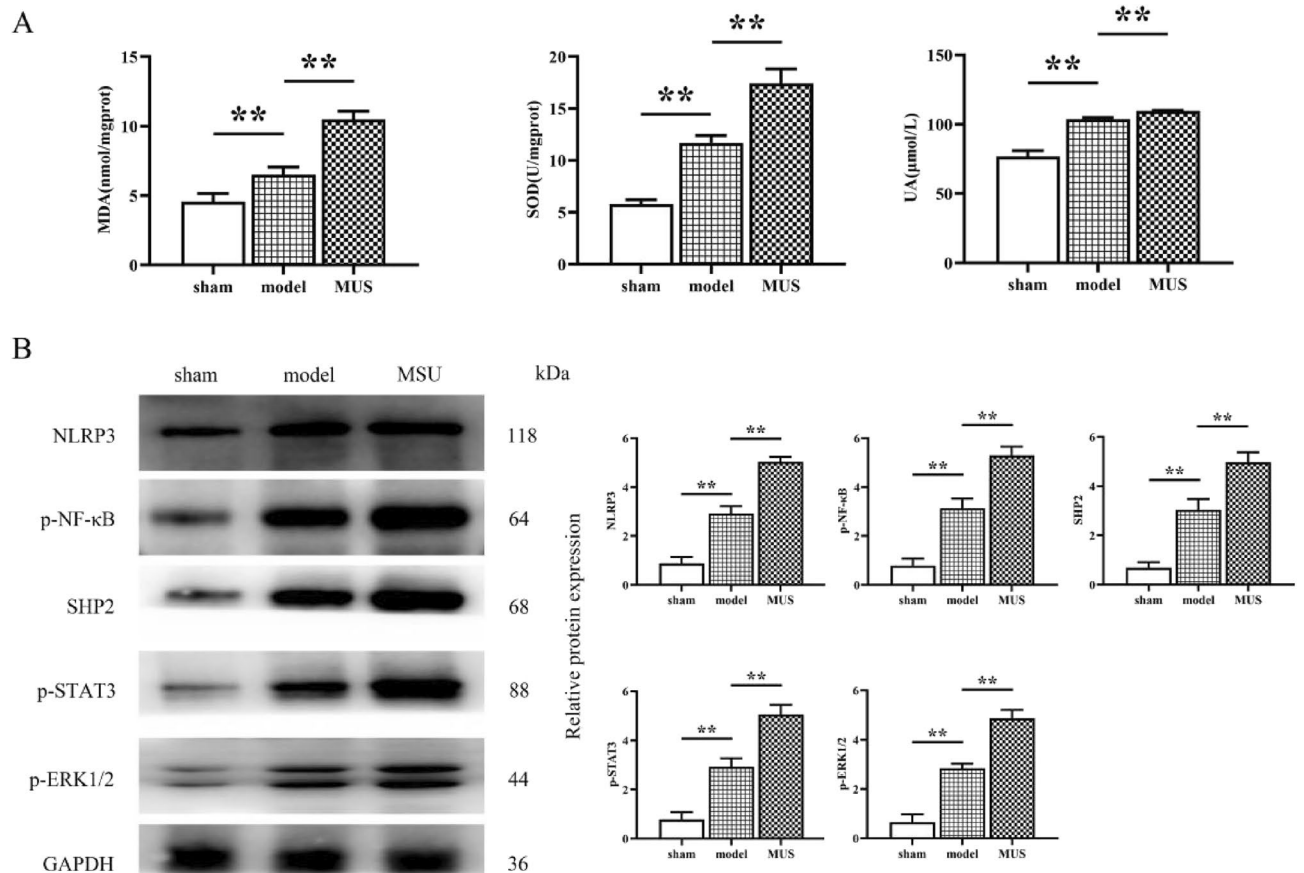


Figure 2. MSU exacerbates renal fibrosis in diabetic nephropathy mice through the ROS/SHP2 pathway. (A) ELISA results of MDA, SOD, and UA in mouse kidneys. (B) Bar graph showing protein expression of NLRP3, p-NF- κ B, SHP2, p-STAT3, and p-ERK1/2 in mouse kidneys using Western Blot. ** $P < 0.01$.

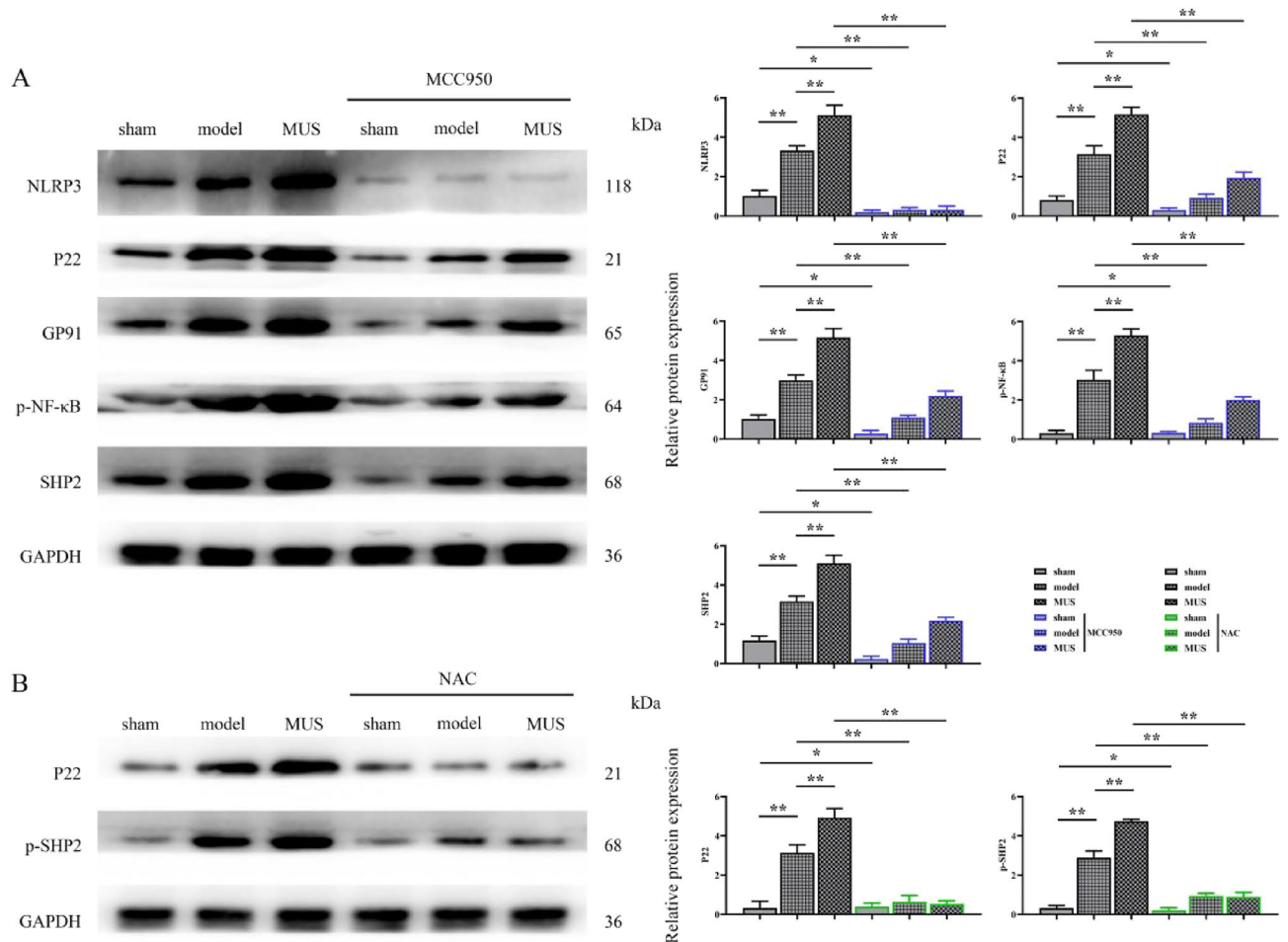


Figure 3. Inhibition of NLRP3 improves ROS and suppresses the expression of p-NF- κ B and SHP2. **(A)** Western blot results of protein expression (NLRP3, P22, GP91, NLRP3, p-NF- κ B, and SHP2) after cultivation in high-glucose medium, MSU, MCC950 (8.1 nM), or 3 mM NAC. **(B)** Bar graph showing protein expression (P22 and SHP2) after cultivation in high-glucose medium, MSU, or NAC using Western Blot. * $P < 0.05$, ** $P < 0.01$.

was an increase in the protein expression levels of NLRP3, P22, NF- κ B, SHP2, and p-SHP2, with no significant difference in the protein expression levels of p-EGFR, p-ERK1/2, and p-STAT3. After SHP2 knockdown, the protein expression levels of NLRP3, P22, and NF- κ B increased under the action of MSU, while there was no significant difference in the protein expression levels of p-SHP2, p-EGFR, p-ERK1/2, and p-STAT3. These results suggest that MSU induces SHP2 activation by activating NLRP3 expression, which further activates the EGFR/ERK1/2/p-STAT3 signaling pathway (Fig. 4).

The effects of SHP2 and MSU on the expression of fibrosis-related proteins in high-glucose-induced L929 cells

To provide additional evidence that MSU exacerbates renal fibrosis through SHP2, we further found that MSU promoted the expression of p-SHP2, p-EGFR, p-STAT3, and Collagen-III proteins. By inhibiting SHP2, we found that shSHP2 suppressed the MSU-induced up-regulation trend of p-SHP2, p-EGFR, p-STAT3 and Collagen-III protein expression. Immunofluorescence results showed that shSHP2 inhibited the expression of the fibrosis marker α -SMA in response to MSU (Fig. 5).

Discussion

Diabetic nephropathy, as a severe complication of diabetes, is showing an increasing trend worldwide²¹. It has significant impact on the quality of life and health of patients and increases the risk of chronic kidney disease and end-stage renal failure²². MSU crystallisation play an important regulatory role in the development of diabetic nephropathy. They induce an imbalance in the SHP2/TGF β pathway in renal fibroblasts by upregulating oxidative stress responses, thereby enhancing the proliferation of fibroblasts and leading to renal fibrotic lesions.

The findings of this study provide important clues for a better understanding of the pathogenesis of diabetic nephropathy. Firstly, MSU crystallisation induce an increase in oxidative stress responses, which may be one of the important reasons for increased proliferation of renal fibroblasts in diabetic nephropathy. Increased oxidative stress disrupts the balance of intracellular redox homeostasis, thereby promoting the proliferation of renal fibroblasts²³.

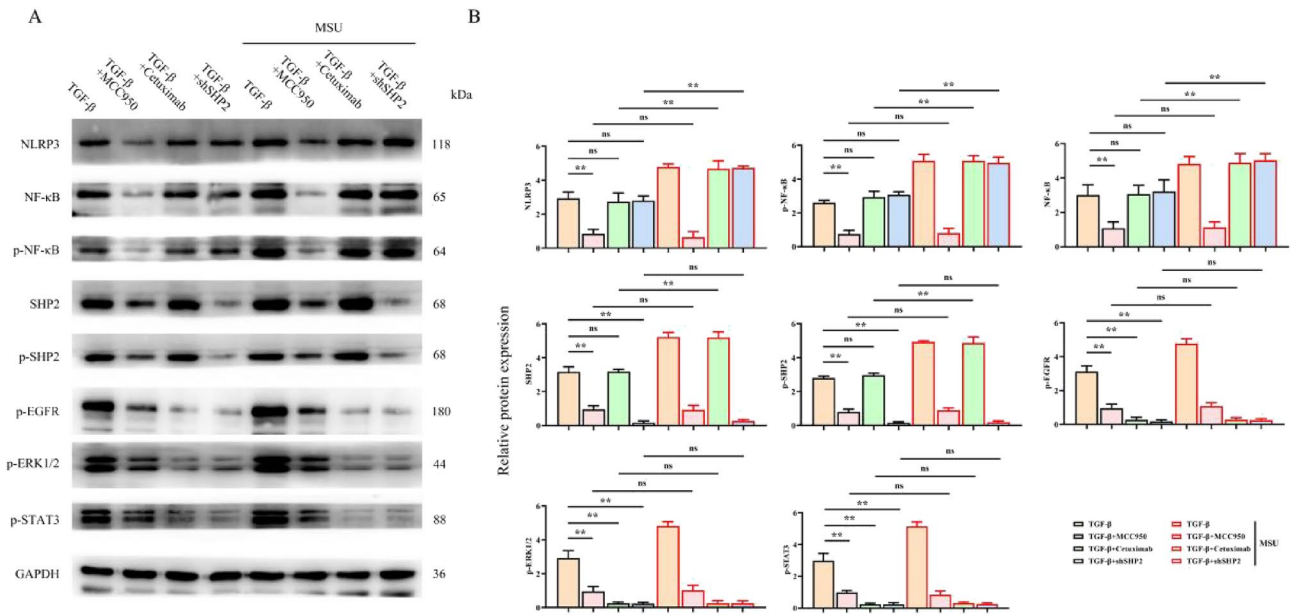


Figure 4. Cetuximab, MCC950A, Sh-SHP2 inhibit MSU-induced expression of ERK1/2 and p-STAT3. (A) Western blot results of protein expression (NLRP3, P22, NF-κB, p-NF-κB, p-SHP2, p-EGFR, p-ERK1/2, and p-STAT3) after cultivation in high-glucose medium, MSU, MCC950 (8.1 nM), or SHP2 knockdown. (B) Bar graph showing protein expression (NLRP3, P22, NF-κB, p-NF-κB, p-SHP2, p-EGFR, p-ERK1/2, and p-STAT3) using Western Blot. *P < 0.05, **P < 0.01, ***P < 0.001.

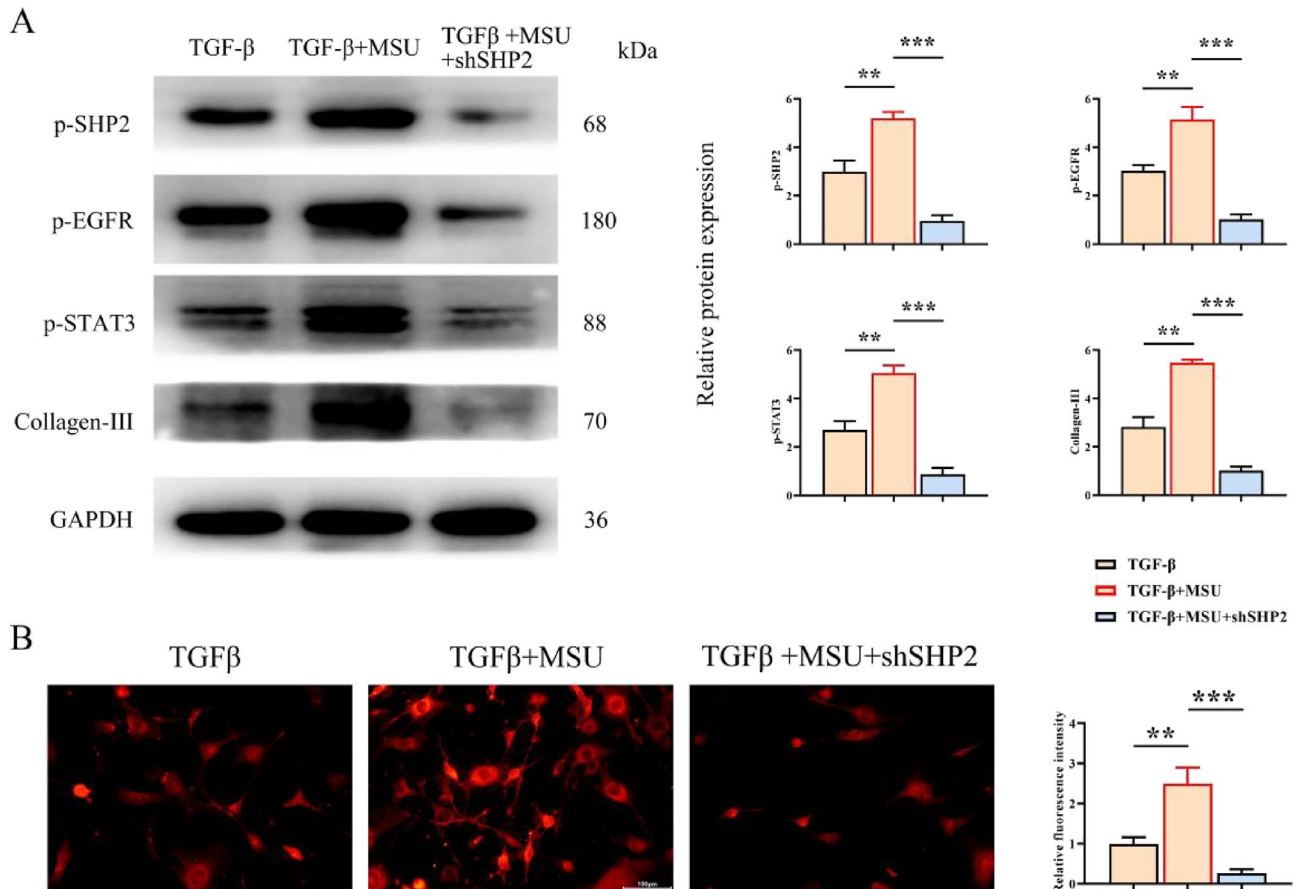


Figure 5. Sh-SHP2 inhibits the expression of renal fibrosis-related proteins induced by MSU. (A) Western blot results of protein expression (p-SHP2, p-EGFR, p-STAT3, and Collagen-III) in L929 cells under high-glucose, TGF-β, MSU, or Sh-SHP2 conditions. (B) Immunofluorescence expression of α-SMA in L929 cells under high-glucose, TGF-β, MSU, or Sh-SHP2 conditions. **P < 0.01, ***P < 0.001.

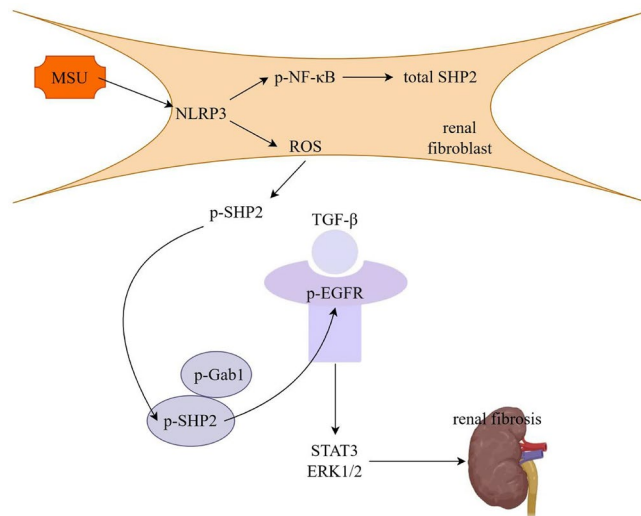


Figure 6. MSU promotes NF- κ B and oxidative stress-induced expression of SHP2 in renal fibroblasts through activation of NLRP3, which in turn enhances the proliferation of fibroblasts within diabetic nephropathy through the TGF β /STAT3/ ERK1/2 signaling path.

MSU crystallisation enhance the proliferation of renal fibroblasts in diabetic nephropathy by regulating the imbalance in the SHP2/TGF β pathway. SHP2 is an important signaling molecule involved in the regulation of various cellular physiological and pathological processes. Studies have shown that SHP2 can be activated by binding with phosphorylated GAB1, and the dissociation of the cytoplasmic GAB1-SHP2 complex and dephosphorylation of GAB1 can activate EGFR²⁴. EGFR promotes the proliferation of renal fibroblasts through the STAT3-ERK1/2 signaling pathway²⁵. This study found that the imbalance in the SHP2/TGF β pathway induced by MSU crystallisation may be one of the key mechanisms leading to renal fibrosis in diabetic nephropathy. Further research can further explore the regulatory mechanisms of the SHP2/TGF β pathway and clarify its role in diabetic nephropathy.

In addition, this study also found that the activation of the NLRP3/ROS signaling pathway may be one of the key factors inducing the upregulation of SHP2 by MSU crystallisation. NLRP3 is an important inflammatory signaling pathway, and in diabetic rats, NLRP3 undergoes oxidative stress through the NF- κ B signaling pathway and increases the expression of inflammatory markers²⁶. ROS is an important intracellular oxidative stress factor, and its effect on SHP2 varies at different H₂O₂ concentrations. Studies by Rima Chattopadhyay have shown that ROS production can mediate SHP2 inactivation²⁷, and a study by Hyunju Park has shown that ROS regulates ROS-induced oxidative stress²⁸. Our study found that ROS functions by promoting the phosphorylation of SHP2 in renal fibroblasts. MSU crystallisation may induce the upregulation of SHP2 by activating the NLRP3/ROS signaling pathway, thereby promoting the proliferation of fibroblasts in diabetic nephropathy. We further explored the interaction between the NLRP3/ROS signaling pathway and MSU crystallisation, as well as the SHP2/TGF β pathway, uncovering the specific regulatory mechanisms in renal fibrosis.

In conclusion, MSU crystallisation enhance the proliferation of renal fibroblasts in diabetic nephropathy by inducing an imbalance in the SHP2/TGF β pathway through upregulation of oxidative stress responses, leading to renal fibrotic changes. This study provides important clues for a better understanding of the pathogenesis of diabetic nephropathy and offers new insights for the development of treatment strategies targeting MSU crystallisation and oxidative stress. Further research is needed to investigate the mechanisms underlying the relationship between MSU crystallisation and uric acid nephropathy, aiming to improve the quality of life and prognosis of patients with diabetic nephropathy (Fig. 6).

Data availability

The authors confirm that the data supporting the findings of this study are available within supplementary materials.

Received: 6 February 2024; Accepted: 10 July 2024

Published online: 31 August 2024

References

- Xue, R. *et al.* Mechanistic insight and management of diabetic nephropathy: recent progress and future perspective. *J. Diabetes Res.* **2017**, 1839809 (2017).
- Li, X. *et al.* Epigenetics in the pathogenesis of diabetic nephropathy. *Acta Biochim. Biophys. Sin.* **54**(2), 163–172 (2022).
- Kanwar, Y. S., Sun, L., Xie, P., Liu, F. Y. & Chen, S. A glimpse of various pathogenetic mechanisms of diabetic nephropathy. *Ann. Rev. Pathol.* **6**, 395–423 (2011).
- Khan, N. U. *et al.* Insights into predicting diabetic nephropathy using urinary biomarkers. *Biochimica et biophysica acta. Proteins and proteomics* **1868**(10), 140475 (2020).

5. Casagrande, V., Federici, M. & Menghini, R. TIMP3 involvement and potentiality in the diagnosis, prognosis and treatment of diabetic nephropathy. *Acta diabetologica* **58**(12), 1587–1594 (2021).
6. Su, H. Y., Yang, C., Liang, D. & Liu, H. F. Research advances in the mechanisms of hyperuricemia-induced renal injury. *BioMed Res. Int.* **2020**, 5817348 (2020).
7. Clebak, K. T., Morrison, A. & Croad, J. R. Gout: Rapid evidence review. *Am. Family Phys.* **102**(9), 533–538 (2020).
8. Preitner, F. *et al.* Urate-induced acute renal failure and chronic inflammation in liver-specific Glut9 knockout mice. *Am. J. Physiol. Renal Physiol.* **305**(5), F786–F795 (2013).
9. Bjornstad, P. *et al.* Role of bicarbonate supplementation on urine uric acid crystals and diabetic tubulopathy in adults with type 1 diabetes. *Diabetes, Obesity Metab.* **20**(7), 1776–1780 (2018).
10. Wang, L., Wang, H. L., Liu, T. T. & Lan, H. Y. TGF- β as a master regulator of diabetic nephropathy. *Int. J. Mol. Sci.* **22**(15), 7881 (2021).
11. Han, Y. *et al.* Reactive oxygen species promote tubular injury in diabetic nephropathy: The role of the mitochondrial ros-txnip-nlrp3 biological axis. *Redox Biol.* **16**, 32–46 (2018).
12. Hsu, M. F., Ito, Y., Afkarian, M. & Haj, F. G. Deficiency of the Src homology phosphatase 2 in podocytes is associated with renoprotective effects in mice under hyperglycemia. *Cell. Mol. Life Sci. : CMLS* **79**(10), 516 (2022).
13. Yang, F. *et al.* Metformin Inhibits the NLRP3 Inflammasome via AMPK/mTOR-dependent Effects in Diabetic Cardiomyopathy. *Int. J. Biol. Sci.* **15**(5), 1010–1019 (2019).
14. Sharma, B. R. & Kanneganti, T. D. NLRP3 inflammasome in cancer and metabolic diseases. *Nat. Immunol.* **22**(5), 550–559 (2021).
15. Zhang, Y., Yang, W., Li, W. & Zhao, Y. NLRP3 inflammasome: Checkpoint connecting innate and adaptive immunity in autoimmune diseases. *Front. Immunol.* **12**, 732933 (2021).
16. Zhang, Y. *et al.* BAFF blockade attenuates DSS-induced chronic colitis via inhibiting NLRP3 inflammasome and NF- κ B activation. *Front. Immunol.* **13**, 783254 (2022).
17. Morgan, M. J. & Liu, Z. G. Crosstalk of reactive oxygen species and NF- κ B signaling. *Cell Res.* **21**(1), 103–115 (2011).
18. Song, S. *et al.* Sestrin2 remedies podocyte injury via orchestrating TSP-1/TGF- β 1/Smad3 axis in diabetic kidney disease. *Cell Death Dis.* **13**(7), 663. <https://doi.org/10.1038/s41419-022-05120-0> (2022).
19. Cheng, J. J. *et al.* Palmatine protects against MSU-induced gouty arthritis via regulating the NF- κ B/NLRP3 and Nrf2 pathways. *Drug Des., Dev. Therapy* **16**, 2119–2132 (2022).
20. Sim, H. J., Kim, M. R., Song, M. S. & Lee, S. Y. Kv3.4 regulates cell migration and invasion through TGF- β -induced epithelial-mesenchymal transition in A549 cells. *Sci Rep.* **14**(1), 2309. <https://doi.org/10.1038/s41598-024-52739-4> (2024).
21. Cheng, Y. *et al.* Endogenous miR-204 protects the kidney against chronic injury in hypertension and diabetes. *J. Am. Soc. Nephrol. : JASN* **31**(7), 1539–1554 (2020).
22. Jin, J., Zhou, T. J., Ren, G. L., Cai, L. & Meng, X. M. Novel insights into NOD-like receptors in renal diseases. *Acta Pharmacologica Sinica* **43**(11), 2789–2806 (2022).
23. Kim, J., Jung, K. J. & Park, K. M. Reactive oxygen species differently regulate renal tubular epithelial and interstitial cell proliferation after ischemia and reperfusion injury. *Am. J. Physiol. Renal Physiol.* **298**(5), F1118–F1129 (2010).
24. Furcht, C. M., Buonato, J. M. & Lazzara, M. J. EGFR-activated Src family kinases maintain GAB1-SHP2 complexes distal from EGFR. *Sci. Signal.* **8**(376), 46 (2015).
25. Liu, N. *et al.* Genetic or pharmacologic blockade of EGFR inhibits renal fibrosis. *J. Am. Soc. Nephrol. : JASN* **23**(5), 854–867 (2012).
26. Shen, Z., Yang, C., Zhu, P., Tian, C. & Liang, A. Protective effects of syringin against oxidative stress and inflammation in diabetic pregnant rats via TLR4/MyD88/NF- κ B signaling pathway. *Biomed. Pharmacother. Biomed. Pharmacotherapie* **131**, 110681 (2020).
27. Chattopadhyay, R., Raghavan, S. & Rao, G. N. Resolvin D1 via prevention of ROS-mediated SHP2 inactivation protects endothelial adherens junction integrity and barrier function. *Redox Biol.* **12**, 438–455 (2017).
28. Park, H., Ahn, K. J., Lee Kang, J. & Choi, Y. H. Protein-protein interaction between caveolin-1 and SHP-2 is dependent on the N-SH2 domain of SHP-2. *BMB Rep.* **48**(3), 184–189 (2015).

Author contributions

Designing the experiment: J.L., J.Z., X.Z., L.T. Performed the experiments: J.L., J.Z., X.Z., L.T. Analyzing the data: J.L., L.T. Prepared the figures and/or tables: J.L., L.T. Drafted the work or revised it critically for important content: J.L., J.Z., X.Z., L.T.

Competing interests

The authors declare no competing interests.

Additional information

Supplementary Information The online version contains supplementary material available at <https://doi.org/10.1038/s41598-024-67324-y>.

Correspondence and requests for materials should be addressed to X.Z. or L.T.

Reprints and permissions information is available at www.nature.com/reprints.

Publisher's note Springer Nature remains neutral with regard to jurisdictional claims in published maps and institutional affiliations.

Open Access This article is licensed under a Creative Commons Attribution-NonCommercial-NoDerivatives 4.0 International License, which permits any non-commercial use, sharing, distribution and reproduction in any medium or format, as long as you give appropriate credit to the original author(s) and the source, provide a link to the Creative Commons licence, and indicate if you modified the licensed material. You do not have permission under this licence to share adapted material derived from this article or parts of it. The images or other third party material in this article are included in the article's Creative Commons licence, unless indicated otherwise in a credit line to the material. If material is not included in the article's Creative Commons licence and your intended use is not permitted by statutory regulation or exceeds the permitted use, you will need to obtain permission directly from the copyright holder. To view a copy of this licence, visit <http://creativecommons.org/licenses/by-nc-nd/4.0/>.

© The Author(s) 2024